

Jet production at next-to-leading order in p+Au collisions at the RHIC^{*}

HE Yun-Cun(何云存)^{1,2;1)} ZHANG Ben-Wei(张本威)^{1,2;2)} WANG En-Ke(王恩科)^{1,2;3)}

¹ Institute of Particle Physics, Central China Normal University, Wuhan 430079, China

² Key Laboratory of Quark & Lepton Physics (Central China Normal University),
Ministry of Education, Wuhan 430079, China

Abstract: We calculate jet productions in p+Au collisions at the RHIC at next-to-leading order with perturbative QCD. Inclusive jet transverse energy spectrum, dijet invariant mass spectrum, dijet angular distribution, and corresponding nuclear modification factors for the three observables in p+Au collisions at $\sqrt{s} = 200$ GeV are given, where the initial-state cold nuclear matter (CNM) effects are included by taking advantage of four parametrization sets of nuclear parton distribution functions (nPDFs) - EPS, nCTEQ, HKN and DS. We demonstrate that inclusive jet transverse energy (E_T) spectrum, dijet invariant mass (M_{JJ}) spectrum with all 4 nPDFs are increased at low E_T or M_{JJ} , whereas at high E_T or M_{JJ} large deviation of results with different nPDFs is observed. It is found that the dijet angular distributions in p+Au collisions do not vary relative to those in p+p collisions for all 4 nPDFs.

Key words: full jet, CNM effects, parametrization sets, nuclear modification factor

PACS: 12.38.Mh, 24.85.+p, 25.75.-q **DOI:** 10.1088/1674-1137/36/11/007

1 Introduction

One of the most important goals of high energy collider experiments is to search for deconfinement quark gluon plasma (QGP). The energetic partons produced in hard process propagating QGP are expected to lose considerable energy and take along abundant information about the early stage. This is called jet quenching, and it is considered one of the strong probes to study the property of QGP [1–4]. The RHIC has observed some phenomena holding jet quenching, such as the suppression of a single hadron at large E_T , the disappearance of back-to-back azimuthal correlations for a dihadron [5], and so on. However, most measurements of them are limited to the leading fragments. As the LHC runs, higher energy and finer acceptance provide new opportunities for full jets [6, 7], which will be an important tool to study the strong interactions and reflect underlying

process more accurately.

Since the ATLAS and CMS collaborations published the displacement of dijet asymmetry as the first measurement of a full jet in AA reactions at the LHC [8, 9], several models exploring the full jet in a hot and dense medium have been proposed [10–16]. Because the initial-state cold nuclear matter (CNM) effects are always present in high-energy nucleus-nucleus collisions, it is important to study jet production in p+A collisions, which may serve as the benchmark of any novel effects due to the formation of the QGP in the final-state of relativistic heavy-ion collisions [17]. In this letter, we start from a single jet cross section, a dijet invariant mass spectrum, and a dijet angular distribution in nucleon-nucleon collisions with perturbative QCD theory. Then we survey these three observables in p+Au collisions at the RHIC by using four parametrization sets of nPDFs, referred to as EPS [18], nCTEQ [19], HKN [20], and DS [21], and

Received 27 February 2012

^{*} Supported by Ministry of Education of China (NCET-09-0411), National Natural Science Foundation of China (11075062, 10825523, 10875052), MOST of China (2008CB317106), NSF of Hubei Province (2010CDA075), MOE and SAFEA of China (PITDU-B08033), and CCNU (CCNU11C01001, QLPL2011P01)

1) E-mail: heyc@iopp.ccnucnu.edu.cn

2) E-mail: bwzhang@iopp.ccnucnu.edu.cn

3) E-mail: wangek@iopp.ccnucnu.edu.cn

©2012 Chinese Physical Society and the Institute of High Energy Physics of the Chinese Academy of Sciences and the Institute of Modern Physics of the Chinese Academy of Sciences and IOP Publishing Ltd

obtain the corresponding nuclear modification factors.

This paper is organized as follows: we establish the baseline in nucleon-nucleon collisions for inclusive jet and dijet productions with perturbative QCD in Section 2. The single jet and dijet observables in p+Au reactions at the RHIC are studied in Section 3. Lastly, we will give a conclusion in Section 4.

2 Single jet and dijet production in nucleon-nucleon collisions

Within the framework of QCD, we can obtain the differential cross section of an inclusive jet at leading order as [22],

$$\frac{d\sigma}{dyd^2E_T} = \sum_{abij} \int_{x_{\text{amin}}}^1 dx_a f_a^A(x_a, Q^2) f_b^B(x_b, Q^2) \frac{2}{\pi} \times \frac{x_a x_b}{2x_a - x_T e^y} \frac{d\sigma}{d\hat{t}}(ab \rightarrow ij), \quad (1)$$

where $f_{a,b}(x_{a,b}, Q^2)$ are the distribution functions of participating partons carrying momentum fractions $x_{a,b}$ in nucleons and Q is the factorization scale. We employ CTEQ6M here. $d\sigma/d\hat{t}$ is the elementary scattering cross section for partons at tree level. We denote $x_T = 2E_T/\sqrt{s}$, $x_b = (x_a x_T e^{-y})/(2x_a - x_T e^y)$, and $x_{\text{amin}} = (x_T e^y)/(2 - x_T e^{-y})$.

Similarly, we can get the differential cross section for a dijet in nucleon-nucleon collisions at leading order,

$$\frac{d\sigma}{dy_1 dy_2 dE_T^2} = \sum_{abij} x_a f_a^A(x_a, Q^2) x_b f_b^B(x_b, Q^2) \times \frac{d\sigma}{d\hat{t}}(ab \rightarrow ij). \quad (2)$$

Here, the momentum fractions x_a and x_b are no longer free as,

$$x_a = \frac{E_T}{\sqrt{s}}(e^{y_1} + e^{y_2}), x_b = \frac{E_T}{\sqrt{s}}(e^{-y_1} + e^{-y_2}). \quad (3)$$

The jets at LO are parent partons, which are inadequate to describe jet physics strictly. At next-to-leading order, jets defined with the radius $R = \sqrt{\Delta y^2 + \Delta\phi^2}$ in rapidity y and azimuthal angle ϕ plane [7] contain more physical information. The cross sections at NLO sum contributions from $2 \rightarrow 2$ processes including NLO virtual corrections and the contributions from $2 \rightarrow 3$ processes are as follows

$$\frac{d\sigma}{dV_J} = \frac{1}{2!} \int d\Phi_2 \frac{d\sigma(2 \rightarrow 2)}{d\Phi_2} S_2(p_1^\mu, p_2^\mu) + \frac{1}{3!} \int d\Phi_3 \frac{d\sigma(2 \rightarrow 3)}{d\Phi_3} S_3(p_1^\mu, p_2^\mu, p_3^\mu), \quad (4)$$

where dV_J and $d\Phi_{2,3}$ represent the phase space of final jets and particles. The functions S_2 and S_3 involve jet finding algorithms for $2 \rightarrow 2$ processes and $2 \rightarrow 3$ processes, respectively. We will calculate jet production at NLO along the development of an EKS jet framework [23].

Our calculation for a single jet at NLO with pQCD in p+p collisions at $\sqrt{s} = 200$ GeV is compared with the STAR experimental data [24] at the RHIC in Fig. 1. It is the result of a jet with the size $R = 0.4$ in the rapidity range $0.2 < |y| < 0.8$ using a mid-point cone algorithm. We find that the cross section is insensitive to the choice of the factorization and renormalization scale Q in the variation from $0.5E_T$ to $2E_T$, and the scale is set $Q = E_T$. The cross section under pQCD has good agreement with STAR data.

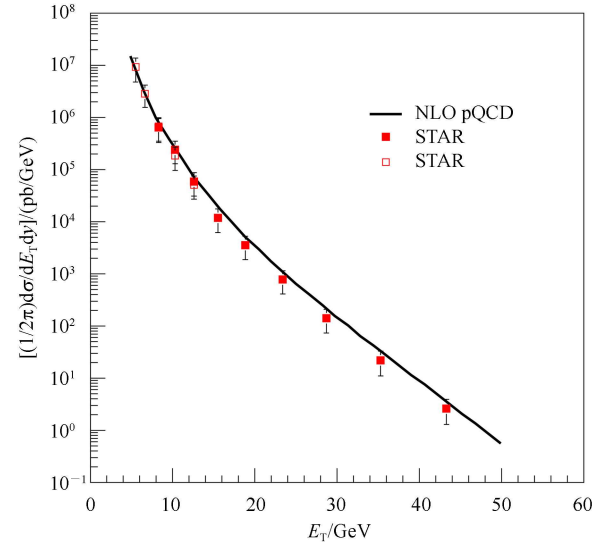


Fig. 1. Single jet spectrum in p+p collisions at $\sqrt{s} = 200$ GeV compared with the experimental results from STAR [24].

The invariant mass spectrum and angular distribution of the dijet are good observables to test the predictions of perturbative QCD and find new physics [25–32]. The first one is defined as $[(\sum p_n^\mu)^2]^{1/2}$ for all the particles in the dijet, and it is related to the transverse energy and rapidity briefly at LO as

$$M_{JJ}^2 = 2E_T^2[1 + \cosh(y_1 - y_2)]. \quad (5)$$

The latter one is an expression of rapidity for the final two jets $\chi = \exp|y_1 - y_2|$.

Experimental measurements for invariant mass spectra and angular distributions of dijets in nucleon-nucleon collisions have been carried out not only on the Tevatron Collider but also at the LHC where the most energetic facility is available presently. The invariant mass spectrum is usually measured in the

bin of maximum rapidity of the two leading jets, $|y|_{\max} = \max(|y_1|, |y_2|)$. The angular distribution is taken in the range of invariant mass M_{JJ} and rapidity of the dijet $y_{JJ} = (y_1 + y_2)/2$.

Figure 2 shows the invariant mass spectrum of the dijet at NLO with the jet size $R = 0.7$ in the rapidity bin $|y|_{\max} < 0.4$ in p+ \bar{p} collisions, which is confronted with D0 data at $\sqrt{s} = 1.96$ TeV [33]. The spectrum drops more than six orders of magnitude in the M_{JJ} range from 200 GeV to 1200 GeV. Fig. 3 demonstrates the angular distributions of the dijet with size $R = 0.4$ in the rapidity $|y_{JJ}| < 1.1$ in p+p collisions, which are compared with ATLAS data at $\sqrt{s} = 7$ TeV [34]. The distributions in three different mass intervals have been tested. The agreement between the numerical and experimental results for

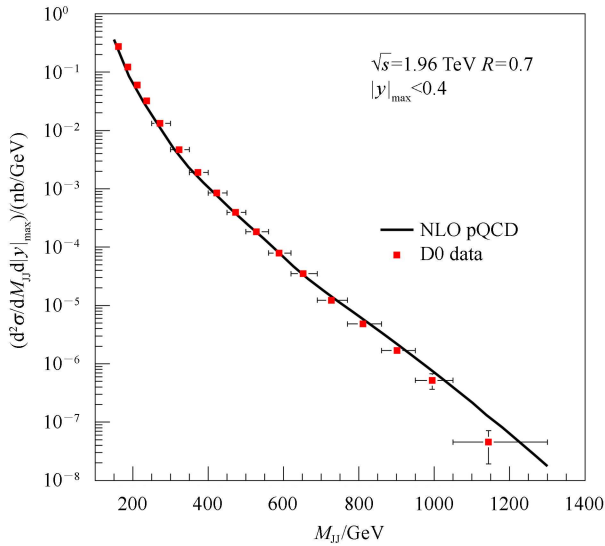


Fig. 2. Dijet invariant mass spectrum in p+ \bar{p} collisions at $\sqrt{s} = 1.96$ TeV compared with the data from D0 collaboration [33].

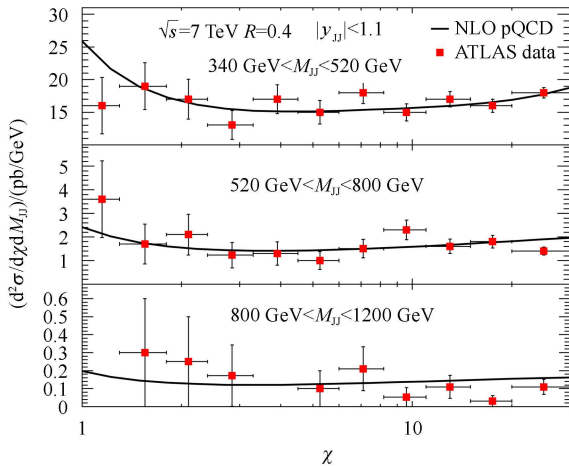


Fig. 3. Dijet angular distribution in p+p collisions at $\sqrt{s} = 7$ TeV compared with the data from the ATLAS collaboration [34].

these two observables has further verified that our pQCD theory is reliable.

3 Single jet and dijet production in p+Au reactions

We investigate jet production in p+Au collisions as a result of initial CNM effects, replacing the parton distribution functions in Eqs. (1), (2) by nPDFs under Glauber Model. We incorporate four different sets of nPDFs (EPS [18], nCTEQ [19], HKN [20], and DS [21]), containing shadowing, anti-shadowing, EMC and fermion motion effects. When the CNM effects are imported, the isospin symmetry for bound protons and neutrons should be taken into account. In order to investigate the CNM effects on jet spectra quantitatively, we will define nuclear modification factors for jet production in minimum bias in the following.

3.1 Single jet production with CNM effects

The nuclear modification factor for a single jet spectrum in p+A collisions relative to the spectrum in p+p collisions is written as a function of the transverse energy as

$$R_{pA}^{E_T} = \frac{d\sigma_{pA}/dE_T}{\langle N_{\text{bin}} \rangle d\sigma_{pp}/dE_T}, \quad (6)$$

where $\langle N_{\text{bin}} \rangle$ in the denominator denotes pairs of participating collisions. It is $\langle N_{\text{bin}} \rangle = \int d^2r t_A(\mathbf{r})$ in p+A collisions and $t_A(\mathbf{r})$ is the thickness function in the transverse plane.

Figure 4 reveals the rescaled spectra of a single jet and nuclear modification factors as a function of the transverse energy in p+Au collisions at RHIC with different nPDFs. It presents the results for a single jet with size $R = 0.5$ in the rapidity $0.2 < |y| < 0.8$. We can see the rescaled spectra are driven up by CNM effects under all the nPDFs parameterization sets in the range before 30 GeV. In the area of final transverse energy after 30 GeV, EPS and nCTEQ nPDFs sets depress the spectra first, and then boost the spectra again. However HKN and DS sets enhance the spectra all the time, and the result under the DS set is especially striking. The discrepancy of nuclear modification factors with different nPDFs parameterization sets is obvious.

3.2 Dijet production with CNM effects

The nuclear modification factors for dijet production are defined similarly with those for a single jet.

We express the nuclear modification factors for invariant mass spectrum $d^2\sigma_{pA}/dM_{JJ}d|y|_{\max}$ and angular distribution $d\sigma_{pA}/\sigma_{pA}d\chi$ of a dijet in p+A collisions, respectively,

$$R_{pA}^{M_{JJ}} = \frac{d^2\sigma_{pA}/dM_{JJ}d|y|_{\max}}{\langle N_{\text{bin}} \rangle d^2\sigma_{pp}/dM_{JJ}d|y|_{\max}}, \quad (7)$$

$$R_{pA}^{\chi} = \frac{d\sigma_{pA}/\sigma_{pA}d\chi}{d\sigma_{pp}/\sigma_{pp}d\chi}. \quad (8)$$

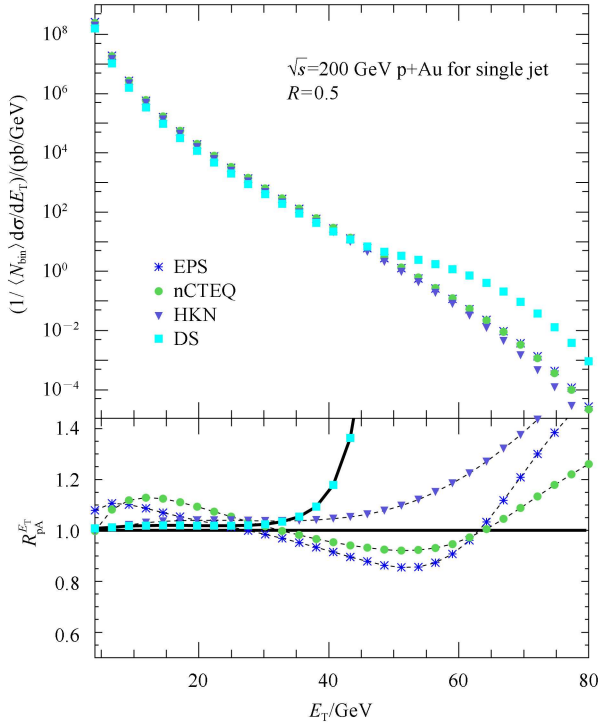


Fig. 4. Single jet rescaled spectra in p+Au and their nuclear modification factors under different sets of nPDFs.

Figure 5 indicates the rescaled invariant mass spectra of a dijet and the relevant nuclear modification factors in p+Au collisions at the RHIC with four sets of nPDFs. They are spectra of a dijet with the jet size $R=0.4$ in the rapidity bin $0.3 < |y|_{\max} < 0.8$. The rescaled invariant mass spectra in p+Au collisions are increased due to the CNM effects with all 4 nPDFs parameterization sets when the dijet mass is lower than about 65 GeV. In the invariant mass range from 65 GeV to 150 GeV, the CNM effects with EPS and nCTEQ sets become suppressions, but those with HKN and DS sets are still enhancements, particularly for DS. In the middle rapidity, we can estimate $M_{JJ} \sim 2E_T$ at LO from Eq. (5). The intervals of shadowing and anti-shadowing effects for the dijet invariant mass spectrum are consistent with those for single jet spectrum, as shown in Fig. 4. The discrimination of nuclear modification factors for dijet in-

variant mass spectra utilizing four nPDFs sets is also visible.

Shown in Fig. 6 are the nuclear modification factors for angular distributions of a dijet with $R=0.4$ in the mass interval $35 \text{ GeV} < M_{JJ} < 50 \text{ GeV}$ in p+Au collisions at the RHIC. The nuclear modification factors for dijet angular distributions do not vary with angle χ at all and the factors are equal to unity. Dijet

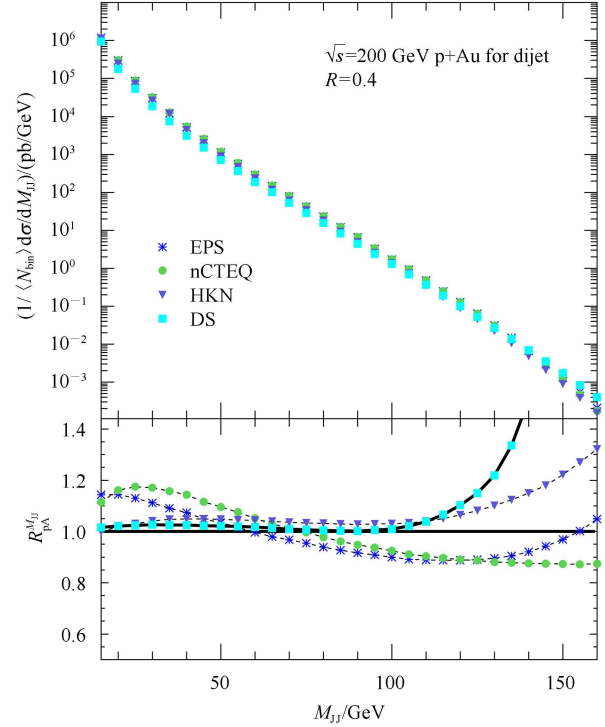


Fig. 5. Dijet rescaled invariant mass spectra in p+Au and their nuclear modification factors under different sets of nPDFs.

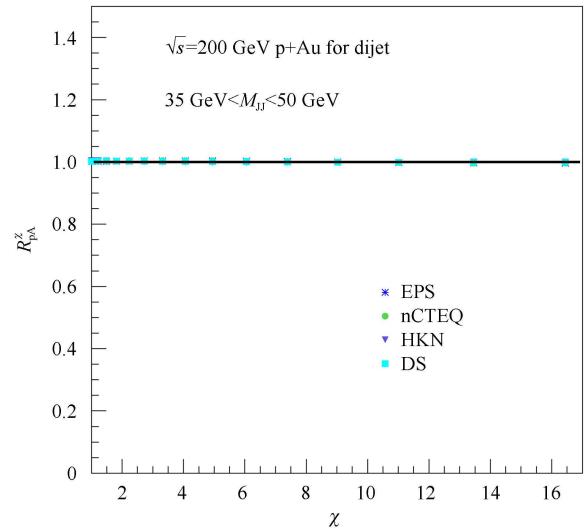


Fig. 6. Nuclear modification factors for angular distributions of dijet in p+Au under different sets of nPDFs.

angular distributions in p+Au collisions are just the same as those in nucleon-nucleon reactions. This illustrates that dijet angular distributions are not affected by the initial CNM effects.

4 Conclusion

Jet production in relativistic heavy-ion collisions can provide detailed information of parton scattering and propagation in the QCD medium. The study of jet observables in p+A collisions is indispensable because it gives the baseline of any final-state effects expected in high-energy nuclear reactions.

In this paper, we explore the inclusive jet and di-

jet observables in p+Au collisions at the RHIC on account of CNM effects, combining the cross sections at NLO in p+p collisions with four different parameterization nPDFs (EPS, nCTEQ, HKN, DS). We illustrate that the rescaled single jet $d\sigma_{pA}/dE_T$ by number of binary collisions with the four nPDFs sets are all enhanced at small and large E_T due to the CNM effects, but the degrees of enhancements show deviations with different sets of nPDFs. The nuclear modification factor of dijet $d\sigma_{pA}/dM_{JJ}$ in p+Au reactions at the RHIC also increases at small M_{JJ} , though at very high M_{JJ} the results with different nPDFs show large variations. The modifications of different nPDFs on $d\sigma_{pA}/dM_{JJ}$ are also distinguishable. The CNM effects on $d\sigma_{pA}/\sigma_{pA}d\chi$ at the RHIC are negligible.

References

- 1 WANG X N, Gyulassy M. Phys. Rev. Lett., 1992, **68**: 1480–1483; Gyulassy M, Vitev I, WANG X N et al. arXiv:nucl-th/0302077
- 2 Baier R, Dokshitzer Y L, Mueller AH et al. Nucl. Phys. B, 1997, **484**: 265–282; Zakharov B G. JETP Lett., 2001, **73**: 49–52; Armesto N, Salgado C A, Wiedemann U A. Phys. Rev. D, 2004, **69**: 114003
- 3 Gyulassy M, Levai P, Vitev I. Phys. Rev. Lett., 2000, **85**: 5535–5538; Vitev I. Phys. Rev. C, 2007, **75**: 064906
- 4 WANG X N, GUO X F. Nucl. Phys. A, 2001, **696**: 788; ZHANG B W, WANG X N. Nucl. Phys. A, 2003, **720**: 429; ZHANG B W, WANG E K, WANG X N. Nucl. Phys. A, 2005, **757**: 493
- 5 Adler C et al. (STAR collaboration). Phys. Rev. Lett., 2003, **90**: 082302
- 6 Campbell J M, Huston J W, Stirling W J. Rept. Prog. Phys., 2007, **70**: 89
- 7 Ellis S D, Huston J, Hatakeyama K et al. Prog. Part. Nucl. Phys., 2008, **60**: 484
- 8 Aad G et al. (Atlas collaboration). Phys. Rev. Lett., 2010, **105**: 252303
- 9 Chatrchyan S et al. (CMS collaboration). Phys. Rev. C, 2011, **84**: 024906
- 10 QIN G Y, Muller B. Phys. Rev. Lett., 2011, **106**: 162302
- 11 Lokhtin I P, Belyaev A V, Snigirev A M. Eur. Phys. J. C, 2011, **71**: 1650
- 12 YOUNG C, Schenke B, Jeon S et al. Phys. Rev. C, 2011, **84**: 024907
- 13 Vitev I, Wicks S, ZHANG B W. JHEP, 2008, **0811**: 093
- 14 Vitev I, ZHANG B W. Phys. Rev. Lett., 2010, **104**: 132001
- 15 Neufeld R B, Vitev I, ZHANG B W. Phys. Rev. C, 2011, **83**: 034902
- 16 HE Y, Vitev I, ZHANG B W. arXiv:1105.2566
- 17 HE Y, ZHANG B W, WANG E. Eur. Phys. J. C, 2012, **72**: 1904
- 18 Eskola K J, Paukkunen H, Salgado C A. JHEP, 2008, **0807**: 102
- 19 Schienbein I, YU J Y, Kovarik K et al. Phys. Rev. D, 2009, **80**: 094004
- 20 Hirai M, Kumano S, Miyama M. Phys. Rev. D, 2001, **64**: 034003; Hirai M, Kumano S, Nagai T H. Phys. Rev. C, 2004, **70**: 044905; Phys. Rev. C, 2007, **76**: 065207
- 21 de Florian D, Sassot R. Phys. Rev. D, 2004, **69**: 074028
- 22 Owens J. F. Rev. Mod. Phys., 1987, **59**: 465
- 23 Kunszt Z, Soper D E. Phys. Rev. D, 1992, **46**: 192
- 24 Abelev B I et al. (STAR collaboration). Phys. Rev. Lett., 2006, **97**: 252001
- 25 Eichten E, Lane K D, Peskin M E. Phys. Rev. Lett., 1983, **50**: 811
- 26 Eichten E, Hinchliffe I, Lane K D et al. Rev. Mod. Phys., 1984, **56**: 579; 1986, **58**: 1065
- 27 Lane K D. arXiv:hep-ph/9605257
- 28 Arkani-Hamed N, Dimopoulos S, Dvali G R. Phys. Lett. B, 1998, **429**: 263
- 29 Atwood D, Bar-Shalom S, Soni A. Phys. Rev. D, 2000, **62**: 056008
- 30 Dienes K R, Dudas E, Gherghetta T. Nucl. Phys. B, 1999, **537**: 47
- 31 Pomarol A, Quiros M. Phys. Lett. B, 1998, **438**: 255
- 32 CHEUNG K M, Landsberg G L. Phys. Rev. D, 2002, **65**: 076003
- 33 Abazov V M et al. (D0 collaboration). Phys. Lett. B, 2010, **693**: 531
- 34 Aad G et al. (Atlas collaboration). Eur. Phys. J. C, 2011, **71**: 1512